A Synthesis Plug-in for Steady and Unsteady Loading and Thickness Noise Auralization

Siddhartha Krishnamurthy[1]
NASA Langley Research Center, Hampton, VA, 23681, USA

Brian C. Tuttle[2]
Analytical Mechanics Associates Inc., Hampton, VA, 23681, USA

Stephen A. Rizzi[3]
NASA Langley Research Center, Hampton, VA, 23681, USA

This paper describes the development and architecture of a plugin for the NASA Auralization Framework that synthesizes rotor sound pressures sample by sample for simulated propagation to auralize rotorcraft flyovers. The main component of the plugin is a preprocessor that synthesizes sound pressures before propagation methods are called. Rotor blade loadings, motion, and geometry data from various tools serve as input to the plugin. Farassat formulation 1A, a solution to the Ffowcs Williams-Hawkings equation, is used for the sound pressure calculations. Use of the plugin is demonstrated with two examples of steady periodic sound synthesis, but the synthesis method and preprocessor architecture described in this paper are also applicable to unsteady periodic and aperiodic sound syntheses.

I. Introduction

This paper is directed at a new capability to synthesize rotor/propeller loading and thickness noise within the NASA Auralization Framework (NAF) [1]. Auralization is a technique for creating audible sound files from numerical data [2]. Here, it refers to the combined process of source noise synthesis, propagation to a ground observer, and receiver simulation [3]. The auralizations created with this capability are intended to be used in human subject tests to assess noise impact. This is particularly important for future air vehicles for which flight recordings are not available.

The synthesis process in this work generates pressure time histories near a rotorcraft noise source based on a source noise definition. In general, source noise definitions can originate from various methods, including computational analyses or ground and flight test measurements when available. This work focuses on computational analyses. In particular, computed rotor blade loadings, motion, and geometry data serve as input to Farassat formulation 1A [4], a solution to the Ffowcs Williams-Hawkings (FW-H) equation [5]. Blade loadings refer to surface pressures and may be represented in compact (line load) or noncompact forms. Synthesized pressure time histories are often predicted at discrete points on a hemisphere at some radial distance from the source [6, 7]. In contrast, this work synthesizes sound along a trace with a time-varying emission angle at some fixed distance from the source. The prediction point that follows this trace is referred to as a tracking observer [8]. The emission angle is dictated by the instantaneous path between the source and the ground observer at the time of emission. The six degree-of-freedom (6DoF) flight path is defined by the source position (x,y,z) and its attitude (heading, roll, pitch). In this work, the ground observer position is considered as fixed, and a straight line propagation path is used. Propagation effects, such as atmospheric absorption and Doppler effects, are subsequently applied to the synthesized sound to obtain a pseudorecording at the ground observer.

---

[1] Research Engineer, Structural Acoustics Branch, Member AIAA.
[2] Scientist III.
[3] Senior Researcher for Aeroacoustics, Aeroacoustics Branch, Fellow AIAA.

The synthesized source noise may be either steady or unsteady. Steady source noise is periodic and offers computational efficiency in defining the source noise by limiting the calculation of blade loading to either one blade passage or one revolution. Unsteady noise may be either periodic, as in the case of a periodic inflow, or aperiodic. Aperiodic loadings may occur on short timescales, for example at the blade passage frequency, or on longer timescales of seconds, such as those associated with aircraft maneuvers. It will become apparent that the additional burden between steady and unsteady sources is on the input data requirements, not on the auralization itself. A motivation for this work is the need to make the synthesis method [8] amenable to source noise definitions stemming from different computer codes, so that the auralization capability can be exercised on rotor and propeller driven aircraft, including helicopters and urban air mobility vehicles.

A. Previous Work

Recent work in Ref. [8] described a process to synthesize steady and unsteady rotor loading and thickness noise at the instantaneous emission angles between the source and the receiver. That paper demonstrated an auralization of a helicopter maneuver involving accelerations and attitude changes with the inclusion of atmospheric absorption and ground reflection. A sound file of the auralization is available for download [9]. The synthesis process is called "F1A Synthesis" because sound for each instantaneous emission angle is computed sample by sample using Farassat's formulation 1A (F1A) [4]. This process avoids interpolation artifacts in a previous additive synthesis method that used sound pressure predictions on a hemisphere around a source at a discrete set of regularly spaced emission angles [6]. To avoid those artifacts, Ref. [8] coupled tools for generating blade loadings and motions with methods to compute sound pressures. In that work, the Fundamental Rotorcraft Acoustic Modeling from Experiments (FRAME) program [10] generated data that were used by the second generation Aircraft NOise Prediction Program (ANOPP2) [11] to predict and synthesize sound pressures using F1A. The NAF [1] subsequently applied propagation effects to the synthesized sound from ANOPP2. The NAF was also used to generate the instantaneous emission angles for the F1A calculation.

Leveraging the prototyped F1A Synthesis method from Ref. [8], the work described in the following sections of this paper develops an F1A synthesizer into a more versatile NAF plugin. The NAF provides a C++ language application programming interface (API) for users to write their own user code, and this capability is used to create an F1A Synthesis plugin. The plugin supplements other NAF plugins that have previously been developed for synthesis of broadband, narrowband, and steady periodic noise. Section II gives a conceptual overview of the synthesis process. Sections III and IV delve into the software architecture for auralization and the F1A Synthesis plugin. Sections V and VI demonstrate the synthesis of rotor flyover sounds using the plugin.

II. Synthesis Methods

A. Helicopter Flyover Overview

To setup a helicopter flyover auralization, paths for the helicopter and ground observer are specified as a function of time. For this work, the ground observer is stationary.

Sound propagates along a path with an emission angle defined by the helicopter flight path and the ground observer position. For this work, as well as in Refs. [6, 8], sound pressure at a particular emission angle is computed using Farassat's formulation 1A (F1A). Rotor geometry, blade loadings, and blade motion serve as input to the sound prediction calculations.

B. Additive Synthesis Using Discrete Data

Figure 1 depicts the method of additive synthesis used for previous auralizations of moving rotorcraft [6, 7, 12, 13]. The method applies to steady and unsteady periodic loadings. Here, F1A is used to calculate rotor blade passage sound pressures at discrete spatial points on a source hemisphere around the rotorcraft. Intersection of lines on the hemisphere mesh represent the discrete spatial points, or emission angles, where blade passage signals are predicted. A predicted blade passage signal at each discrete emission angle is decomposed into N harmonics of the blade passage frequency (BPF) using a discrete Fourier transform, in which $N = T \times f_s/2$, assuming $T \times f_s$ is an even number. Here, T is the period of the blade passage, and f_s is the sample rate of the blade passage data. Each harmonic, i of N, consists of a constant magnitude, A_i, and constant phase ψ_i. In Figure 1, the emission angle from source to ground observer at time $t = t_1$ is exactly at a discrete emission angle. An additive synthesis technique is applied to compute the sound pressure at time t_1 using the exact predicted values for magnitude and phase of each harmonic.

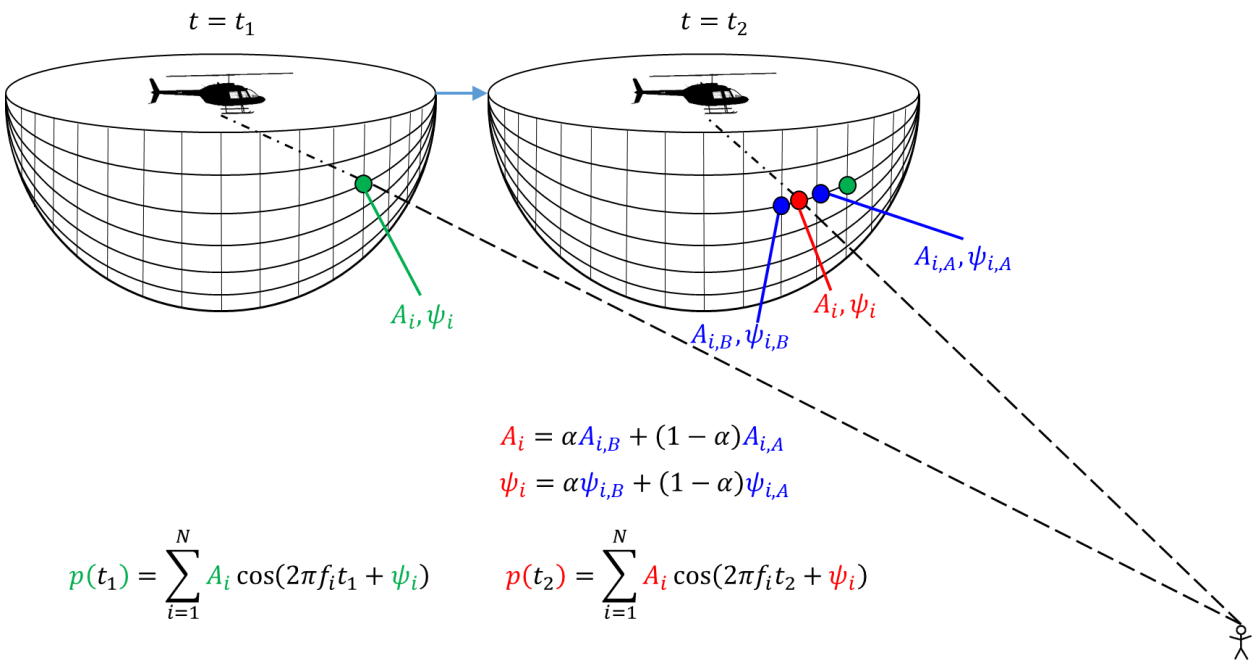

Figure 1. Discretized source hemisphere for periodic additive synthesis.

As the rotorcraft moves relative to the ground observer, the emission angle to the observer varies between discrete emission angles on the source hemisphere. At time step $t = t_2$ in Figure 1, the emission angle from source to observer is between discrete emission angles where blade passages are predicted. The harmonic magnitudes and phases at this point are found by interpolating over the harmonic magnitudes and phases computed at the surrounding discrete emission angles with an appropriate choice for α where $0 \leq \alpha \leq 1$. The additive synthesis is then applied on the interpolated values to compute the sound pressure at time t_2.

This synthesis technique is implemented as an advanced NAF plugin for periodic additive sound synthesis [1]. References [6, 7] also describe the interpolation process. The synthesized sound pressure at each time step is then propagated to a ground observer to complete the auralization.

Synthesis according to this approach has certain drawbacks. One drawback is that an insufficiently refined discretization of the source hemisphere relative to the source directivity can result in artifacts in the auralization. Using a finer discretization may be limited by computational capabilities such as available memory. Another drawback is that synthesizing aperiodic signals using interpolation becomes more challenging. See Refs. [7, 12] for examples.

C. F1A Synthesis

Figure 2 illustrates the new synthesis method for the NAF, F1A Synthesis, for synthesizing sound pressures without interpolation of harmonic magnitudes and phases. Here, F1A is used to compute the source noise at each time sample at the instantaneous emission angle between the source and the ground observer. Like the source noise hemisphere, the F1A calculation occurs at some constant radius from the source emission position. As the calculation point is determined at each sample instant, interpolation of the sound pressure magnitude and phase is avoided. In Figure 2, sound pressures at times t_1 and t_2 are computed directly from F1A. Both periodic and aperiodic signals may be computed with F1A Synthesis.

A tracking observer is generated as the F1A calculation continues at each time sample. Figure 2 shows the calculation being performed at just two time samples that have a large time interval between them for illustration purposes. As the sample interval is reduced and the flyover is extended in time, many points at a fixed radius will be formed along the propagation path between the source emission position and the ground observer. Taken together over time, these points generate a spatial track that is illustrated with the dotted solid black trace in Figure 3 between the beginning (green circle) and end (red circle) points. The dotted solid black trace is the set of points defining the tracking observer. Sound pressure is calculated with F1A at each point along the tracking observer.

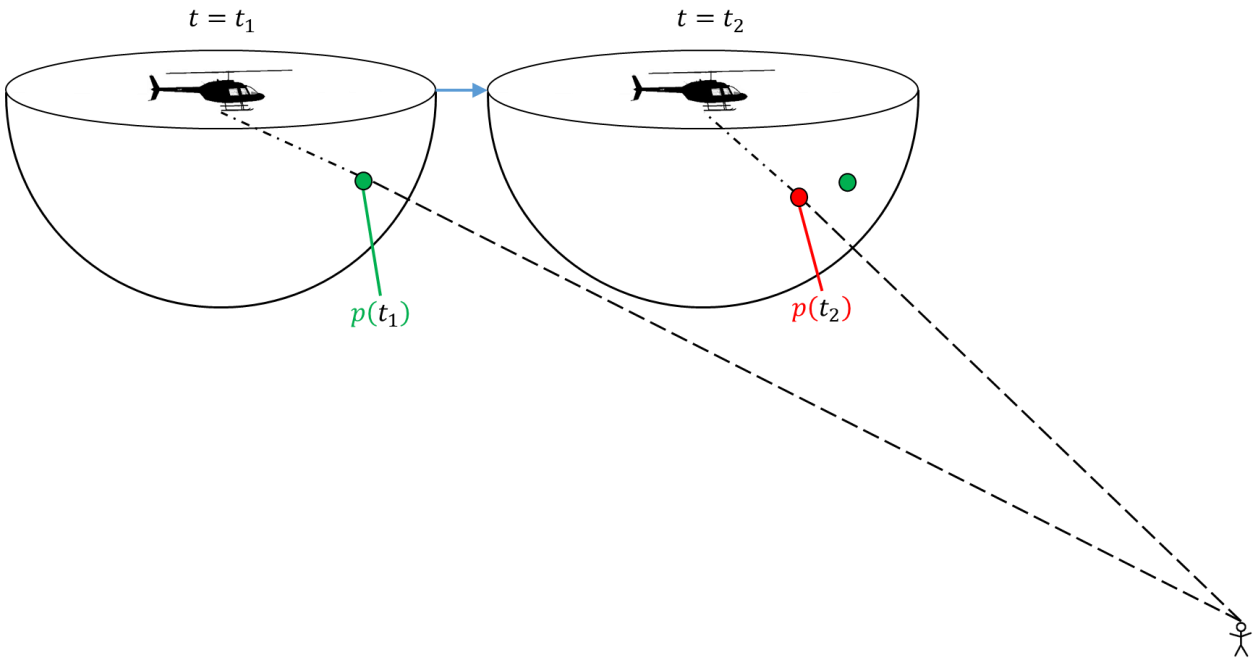

Figure 2. Synthesis method of directly computing sound pressures at each sample.

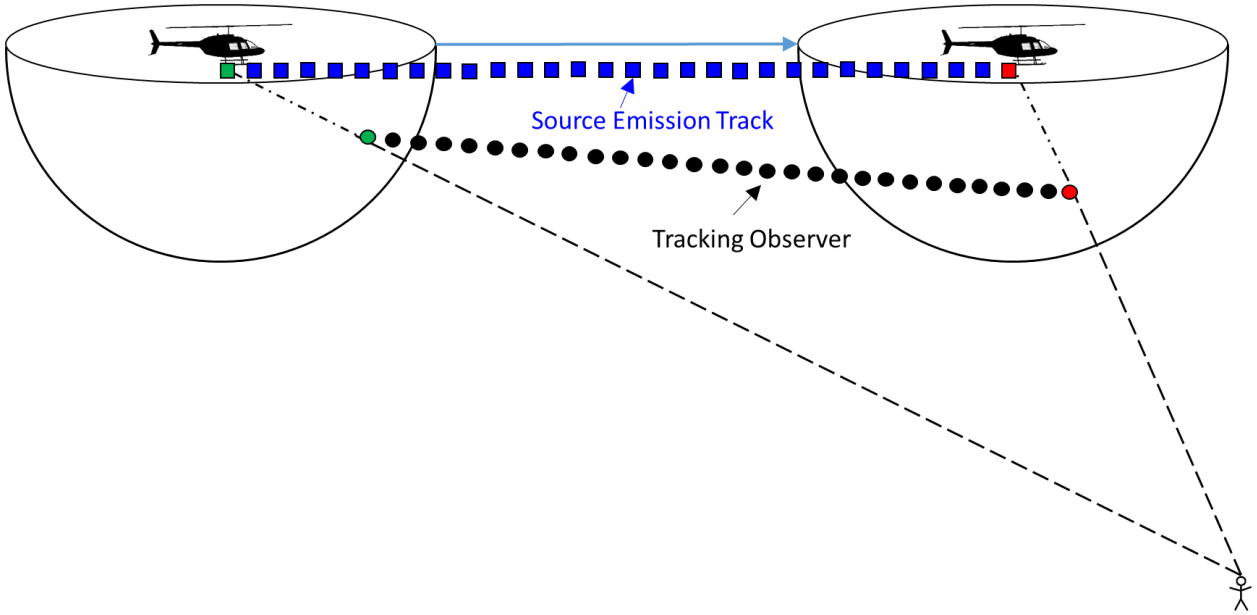

Figure 3. Creation of tracking observer.

The dotted solid blue trace in Figure 3 is the set of source emission positions, or source emission track, which forms, like a trail of breadcrumbs, as the source moves. Each point on the source emission track is paired with a tracking observer point that lies along the propagation path from emission point to ground observer. The green and red squares at the beginning and end of the source emission track propagate sound pressure samples to the green and red circles on the tracking observer, respectively. Since the tracking observer points are formed at a constant distance from the source, there is a constant propagation delay between each pair of points on the source emission track and the tracking observer. This approach avoids Doppler frequency shifts. However, convective amplification effects [14] from rotor translation will be present in the calculations at the tracking observer. Defining the tracking observer as in Figure 3 improves on the F1A Synthesis approach in Ref. [8]. In Ref. [8], a Doppler frequency shift was produced because the time delay between emission and reception was not kept constant.

Multiple tracking observers may exist for an auralization. The illustrations in Figures 1-3 show a single direct propagation path from source emission positions to ground assuming a single noise source. If multiple noise sources exist, as is the case with a multirotor vehicle, a separate tracking observer is needed for each source. In addition, reflected paths, which are not shown, would form another set of emission angles from source emission track to ground and would necessitate creation of more tracking observers, one for each path associated with each source. As an example, if three rotors existed on a vehicle and the propagation involved a direct and reflected path, six tracking observers would be needed, two for each source. In addition, three source emission tracks would be needed to generate the tracking observers.

One may directly synthesize sound pressures at the ground observer instead of at the tracking observer, but propagation effects will need to be applied as post-processing of sound pressure predictions. In Refs. [15, 16, 17, 18], unsteady aperiodic noise of maneuvering helicopters was directly synthesized at the ground observer at each time sample. The sound pressures, however, did not include the effects of atmospheric absorption or ground reflection. Inclusion of these effects in the method of Refs. [15-18] is not straightforward because the source synthesis and propagation are not treated separately. Use of a tracking observer closer to the source in F1A Synthesis allows propagation effects to be implemented independently of the source noise synthesis, which is beneficial for complex propagation environments.

A drawback to the F1A Synthesis approach is that sound pressures at tracking observer points will need to be recalculated if there are *any* changes to the 6DoF flight path. With the additive synthesis approach using discrete data, the same source noise hemisphere may be stored and used with new flyovers if the helicopter changes its 6DoF flight path as long as the noise hemisphere can still be assumed to represent the source noise, such as for the same maneuvers at different locations.

III. Auralization

Once the sound pressures are generated along a tracking observer, they are propagated to the ground observer as part of the auralization process in the NAF. This flow of information is depicted in Figure 4 along with two components of the F1A Synthesis plugin: the F1A Synthesis Preprocessor and the F1A Synthesis loader. Here, the tracking observer sound pressures computed by the F1A Synthesis Preprocessor, depicted with a green parallelogram, are retrieved by the NAF Synthesis Engine by way of an F1A Synthesis loader. Once retrieved, they enter into the typical NAF time domain auralization process, as shown to the right of the vertical dashed line and described in Ref. [1]. The tracking observer pressure time history is fully computed before it is retrieved by the F1A Synthesis loader in a manner akin to the built-in NAF wavefile loader. Specifically, short segments of pressure time history at the tracking observer (typically 512 samples in length at an audio sampling rate of 44.1 kHz) are supplied by the Synthesis Engine to the sample buffer for propagation to a ground observer

The gain/time delay/filter (GTF) processing engine simulates propagation of synthesized sound to a ground observer. The GTF processor acts according to Path Traverser-specified data associated with spherical spreading loss (negative decibel gain), absolute time delay, and atmospheric and ground plane filters. Based upon the supplied flight trajectory and ground observer location, the Path Finder produces path data from each point on the source emission track to the ground. The Path Traverser determines which segment of the tracking observer time history to propagate using the path data. Source emission tracks and ground observer locations are specified in the NAF Scene and are updated over the simulation time. References [1, 3] discuss the NAF auralization process in more detail.

Multiple paths can exist between the source emission track and ground observer in the presence of ground reflections, urban canyon propagation, or curved-ray propagation [19]. Between the Path Finder and the output of the GTF Processor, the NAF synthesizes and propagates sound for each path, and the propagated path contributions are summed at the ground observer. In Ref. [8], only a single direct path was used from the source to an observer flush with the ground. Section VI of this paper demonstrates synthesis for direct and ground reflected paths for auralization at an observer above the ground, assuming flat terrain and a straight line path in a nonrefracting atmosphere. Separate tracking observer pressure time histories associated with the direct and ground reflected paths are generated.

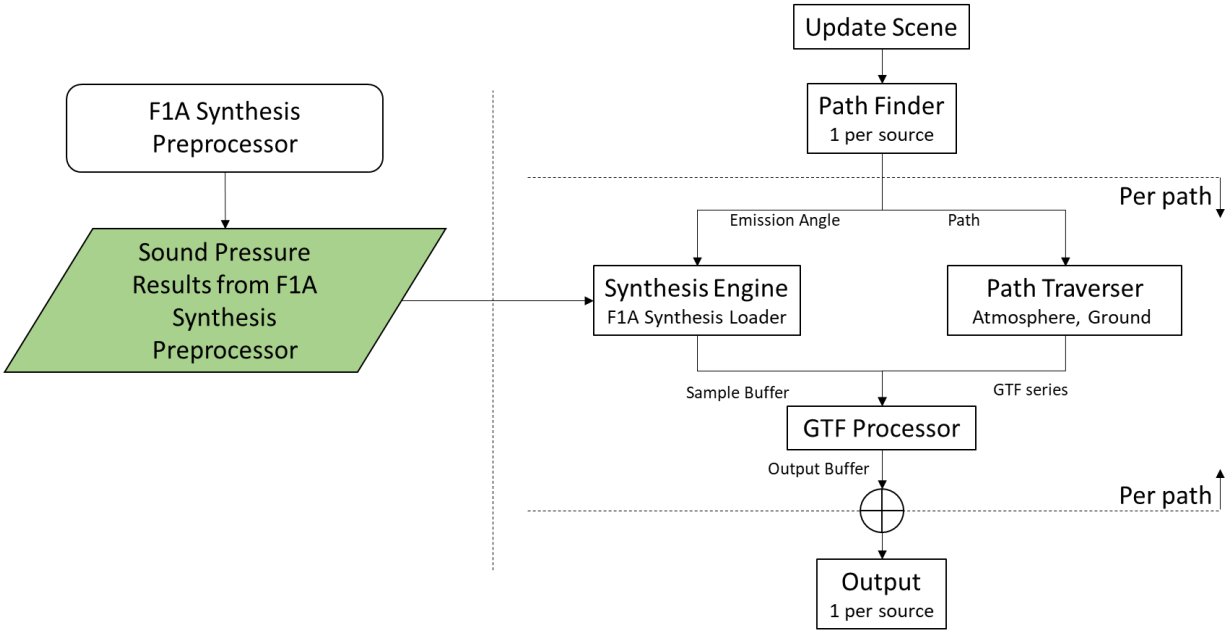

Figure 4. NAF auralization simulation flowchart.

IV. F1A Synthesis Preprocessor

The F1A Synthesis process that generates pressure time histories at a tracking observer is shown in Figure 5. Inputs to the process are blade geometry, blade motion, and the 6DoF flight path. The output is the synthesized pressure time history along the tracking observer that serves as input to the NAF Synthesis Engine in Figure 4. The rounded rectangle blocks in Figure 5 indicate the three main processing blocks of the F1A Synthesis process. Blade loadings, motion, and geometry (BLMG) data are stored in the orange/yellow block. The pink Path Finder block generates the tracking observer positions. The blue ANOPP2: F1A block implements the sound synthesis. In Ref. [8], the ANOPP2: F1A block ran separately from the NAF, which only executed the Path Finder block. In this paper, the NAF F1A Synthesis Preprocessor also controls the ANOPP2: F1A block. This capability leverages an API that allows ANOPP2 functionality to be accessed and executed by external programs [1, 11]. BLMG data are still generated outside of this preprocessor.

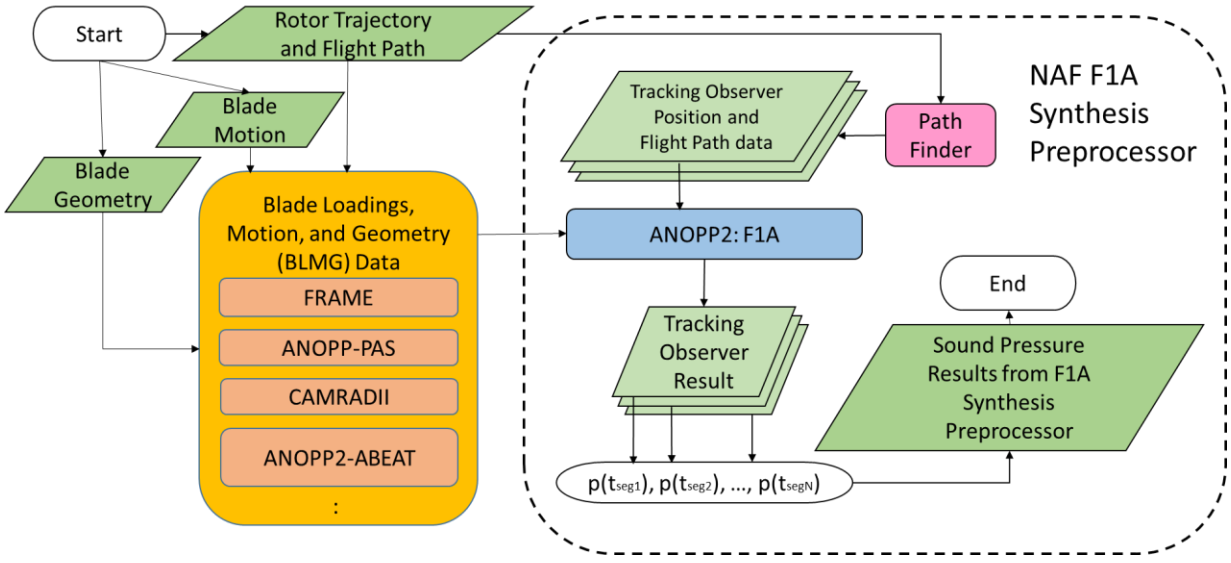

Figure 5. Flowchart for F1A Synthesis.

A. Inputs

The NAF F1A Synthesis plugin runs the preprocessor as part of the setup of the auralization. This setup is run after the environment is established, which includes the atmosphere, sources, observers, and source trajectories. The NAF F1A Synthesis plugin defines a rotor source as a particular type of source that includes information about the rotor geometry as well as the source motion. The first step of the F1A Synthesis Preprocessor is to query the NAF environment to find all rotor sources to apply F1A noise predictions. Once these are identified, each rotor source receives a noise component attribute of thickness, loading, or their sum, total noise, according to user input.

The orange/yellow BLMG block in Figure 5 indicates various blade loadings, motion, and geometry input tools that the preprocessor may use. Only one is used for any particular auralization. Reference [8] used FRAME. As seen in Figure 5, other tools such as the Comprehensive Analytical Rotorcraft Model of the Rotorcraft Aerodynamics and Dynamics (CAMRAD II) [20] program, the ANOPP Propeller Analysis System (ANOPP-PAS) [21], and the newly developed ANOPP2 Blade Element Acoustic Tool (ABEAT) may also provide BLMG input. In this paper, the rotor blades are approximated as compact-line-sources. Blade geometry still includes cross-sectional area. Noncompact data sources, such as those from CFD simulations, can be applied in principle, but they will not be demonstrated in this paper.

BLMG data are provided as a function of time. If steady periodic pressure time history data are synthesized, the BLMG data may be one blade passage in duration. If unsteady periodic pressure time history data are synthesized, one rotor revolution of flight data is required. To synthesize an unsteady aperiodic pressure time history, the duration of the BLMG data needs to be as long as the auralization, hence the particular tool that provides the information must be capable of generating such a time history. Output from the BLMG tools will include an indication of whether sound pressures should be synthesized as being periodic or aperiodic.

B. Generating Tracking Observers

The F1A Synthesis Preprocessor next defines the tracking observers. The right side of the flowchart in Figure 5 shows the NAF Path Finder. In Figure 4, the Path Finder determined the number of sound transmission paths between the rotor source emission track and the ground observer over the course of the rotor's trajectory. The F1A Synthesis Preprocessor uses these same calculations to create a tracking observer for each path, giving it a unique path ID, a beginning and ending time, and a position over time. Rotor and flight 6DoF trajectory provided by the user allow the NAF Path Finder, directed by the preprocessor, to compute the azimuthal and polar emission angle to the ground observer for each path and time step in the auralization. Ground observer position, not shown in Figure 5, is also provided to the Path Finder by the user. The emission angle is then transformed to the source frame of reference. This transformation ensures that changes in heading, pitch, and roll will cause a change in emission angle, even if there is no source translation. The tracking observer position is subsequently calculated using the emission angle and the fixed distance between the source emission track and the tracking observer. The tracking observer positions are output as a time series at a user specified sampling rate. The sampling rate of the tracking observer does not have to match that of the BLMG data. A time vector associated with the tracking observer is relative to the source emission track time. This time vector begins at the propagation delay from the source emission track to the tracking observer. The F1A Synthesis Preprocessor loads both source motion (flight path data) and tracking observer positions into ANOPP2 for the F1A calculation.

Separate source emission tracks and tracking observers must be provided for each rotor on the vehicle. Fixed translation and rotation of the noise source origin with respect to the vehicle origin, typically regarded as its center of gravity, must be provided to the NAF Path Finder to compute the tracking observer positions with respect to the source origin at the time of sound pressure sample emission. If there are vehicle attitude changes involving roll, pitch, and yaw about the center of gravity during a flyover, the origin of each vehicle noise source must be adjusted. Noise source displacement information and vehicle attitude changes exist in the BLMG data, but they are also provided directly to the NAF as part of the rotor trajectory and flight path information.

C. Sound Synthesis

The ANOPP2 F1A Internal Functional Module (AF1AIFM), shown as the ANOPP2: F1A block in Figure 5, computes the noise predictions on the tracking observer in the form of pressure time histories. F1A calculations in ANOPP2 consist of sources (emitters), and observers (receivers). Tracking observers serve as receivers of F1A noise predictions between flyover beginning and ending times. Sound pressures computed along the tracking observer incorporate the directivity of the rotor source as it emits sound toward the ground observer during the flyover. With information about the rotor source trajectory, the tracking observer positions, the blade loading, and the required number of predictions per time, the F1A Synthesis Preprocessor sets up and executes the F1A noise prediction for each tracking observer through its interface with ANOPP2. Atmospheric absorption is not included in the F1A

calculation. The ANOPP2 data structure that holds the pressure time history results of this calculation is stored with the tracking observer. The F1A Synthesis Preprocessor gathers pressure time history data from the tracking observers and sorts them into the appropriate components of loading, thickness, and total noise. It associates each pressure time history with its path ID in order that the NAF Synthesis Engine can identify it by way of the F1A Synthesis loader. The pressure time histories for each noise component are available to be retrieved as needed for auralization.

ANOPP2 requires separate position information for noise sources (emitters) and tracking observers. Multiple source emission tracks and tracking observers exist if a vehicle contains multiple noise sources. While ANOPP2 uses the tracking observer locations, it does not use the multiple source emission tracks directly. Instead, only the vehicle origin x,y,z positions over time are prepared by the preprocessor to define the flight kinematics input for ANOPP2. Fixed translation and rotation of vehicle noise sources from the vehicle origin and vehicle attitude changes are already embedded in the BLMG data given to ANOPP2. Just like the NAF Path Finder, during vehicle attitude changes, ANOPP2 adjusts noise source origin positions with respect to the vehicle center but uses the BLMG data for this operation. This additional step is necessary to make the F1A calculation consistent with the tracking observer data provided by the NAF. Sound pressures are subsequently predicted at tracking observers associated with the adjusted noise source origin positions.

In Figure 5, the tracking observer positions and results are depicted as a multilayer box. Among the features of the plugin is the ability to break the synthesis process into multiple contiguous time history segments, which are referred to as stages, in order to alleviate computer memory limitations. The layers in Figure 5 represent the F1A synthesizer stages for computing pressure time history data over a separate portion of the tracking observer positions. Results of each stage are saved, allowing computer memory to be freed for computations on the subsequent stage. The synthesized pressures from the stages are concatenated at the end of the synthesis.

The NAF F1A Synthesis Preprocessor includes routines to configure the AF1AIFM calculation and to prepare the synthesized sound pressures to be propagated. The preprocessor sets up ANOPP2 to use a source emission sample rate equal to the sample rate provided in the BLMG data. It also sets up ANOPP2 to provide noise prediction data at the tracking observer at a fixed reception sample rate specified by the user. ANOPP2 interpolates sound pressures from the fixed source emission sample rate to the fixed tracking observer sample rate. Before interpolation, emission time points are mapped to a set of reception points unequally spaced in time due to rotor and blade movement. Interpolation between emission and reception in ANOPP2 is different from the harmonic magnitude and phase interpolation described in Section II.B.

Once tracking observer sound pressures are generated, a final synthesis step is to up-sample the tracking observer pressures to the audio sample rate, typically 44.1 kHz, used by the NAF Synthesis Engine. A polyphase interpolator [22], controlled by the preprocessor, is used for the up-sampling. This interpolator includes an antialiasing filter with cut-off frequency slightly below half the tracking observer sample rate.

D. Distance Between Source Emission Track and Tracking Observer

The NAF applies its propagation simulation starting at some small reference distance (typically 1 meter) from the noise source origin at the time of sound sample emission (the source emission track). However, the source noise data (the pressure time history at the tracking observer) should reflect a far field propagating solution that is absent of near field acoustic and hydrodynamic effects. In order for F1A to generate such data, the distance from the source emission track to the tracking observer should be large. Distances in this work ranged from 100 meters to 1000 meters, but distances much greater than 1000 meters reduce the precision of the F1A calculations. Upon input, the NAF adjusts the ANOPP2 synthesis result to account for the difference between the tracking observer distance and the reference distance. This adjustment includes removal of the added spreading loss and application of a time shift to account for propagation delay to the tracking observer. Since the distance from source emission track to the tracking observer is kept constant, a single scalar gain value and a time shift value are applied to all tracking observer pressure samples.

E. Current Status of F1A Synthesis Plugin

All components of the F1A Synthesis plugin have been tested and can be used separately to produce results for multiple noise sources and propagation paths. These results are discussed below. Work is currently being performed to integrate these components so that they can work as a singular entity with the NAF.

V. Synthesis Example

A. Flyover and Calculation Setup

To demonstrate the F1A synthesis NAF plugin, the steady periodic main and tail rotor noise of an AS350 helicopter is synthesized. CAMRAD II serves as the input source for the BLMG data. The synthesized sound is produced to

auralize a straight and level flyover of an observer flush with rigid ground. Figure 6 shows the velocity of the helicopter, the start position, end position, and flyover altitude. The flyover described in Figure 6 has a duration of 20 seconds. The blades of the rotors are modeled as compact-line sources. Noise predictions from the main and tail rotors are first synthesized individually. Distances between the rotor source emission tracks and tracking observers are set to 100 meters for the F1A calculation. After scaling back to one-meter distances, synthesized sounds from both rotors are then propagated to the ground observer and combined to complete the auralization. A uniform atmosphere with pressure of 1 atm, temperature of 285.98 Kelvin, and relative humidity of 70% is used by ANOPP2 for the F1A calculation and by the NAF for propagation. An ambient air density of 1.05 kg/m^3 is also supplied to ANOPP2. At these conditions, the speed of sound is 340.29 m/s.

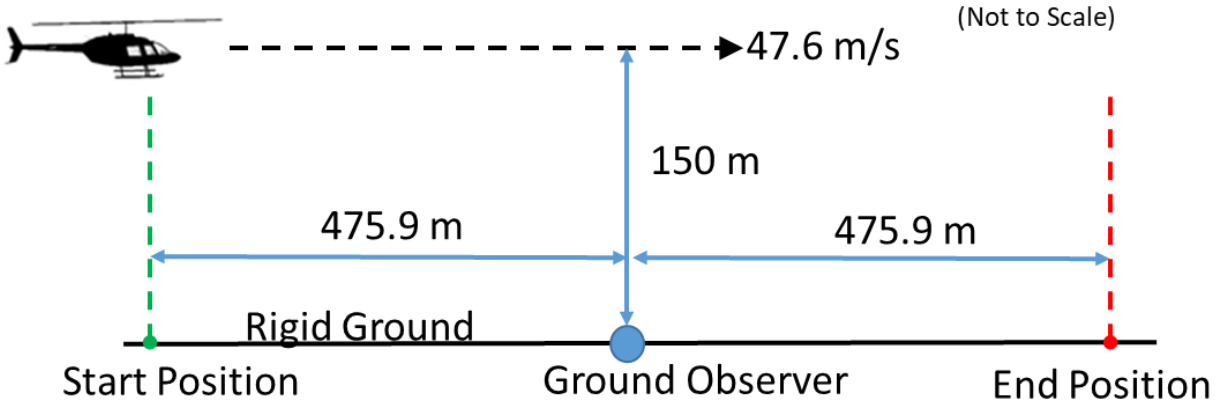

Figure 6. Flyover setup of synthesis example.

The distance values in Figure 6 are given with respect to the vehicle center of gravity. Adjusted distance values are needed with respect to each rotor center to compute the correct tracking observer positions. With the positive x-direction toward the front of the helicopter and the positive z-direction toward the top of the helicopter, the origin of the main rotor is located at $(x, y, z) = (-0.09\ m, 0.00\ m, 1.32\ m)$ with respect to the vehicle center of gravity. The tail rotor origin is located at $(x, y, z) = (-5.95\ m, 0.00\ m, 0.45\ m)$ with respect to the vehicle center of gravity. Not shown in Figure 6 is the attitude of the helicopter. In its trimmed condition, the helicopter has a roll, pitch, and yaw of 1.94 degrees, -2.75 degrees, and 0.00 degrees, respectively, about its center of gravity. The NAF Path Finder calculates emission angles from each rotor center to the ground observer after accounting for rotor center positions and vehicle attitude with respect to the vehicle center of gravity. The emission angles along with the constant distances from source emission tracks determine tracking observer positions.

CAMRAD II provided periodic blade loading data at different sample rates for the main and tail rotors. The main rotor blade loading data sample rate is 1586 Hz, and the tail rotor blade loading data sample rate is 8397 Hz. These sample rates are used to predict emission sound pressures. The tracking observer sample rate is set to 8820 Hz for both the main and tail rotor synthesis.

B. Synthesis Results

Figure 7 shows the separate F1A Synthesis results for the AS350 helicopter main and tail rotor tracking observers for the flyover in Figure 6. The thick blue trace is the sound pressure envelope of the main rotor. The thin red trace is the sound pressure envelope of the tail rotor. The results in Figure 7 have large pressure values because they represent the noise at the 1 meter reference distance. Separate blue and red traces, for the main and tail rotors, respectively, are shown for the elevation and azimuth emission angles to the ground observer. There is a slight offset in the emission angles between the two rotors. The roll of 1.94 degrees about the vehicle center of gravity causes the azimuth emission angles to be slightly different. If the roll was 0 degrees, the azimuth emission angles would be 0 degrees for both rotors. Both roll and pitch about the vehicle center of gravity and rotor center displacements cause the elevation emission angles to be different.

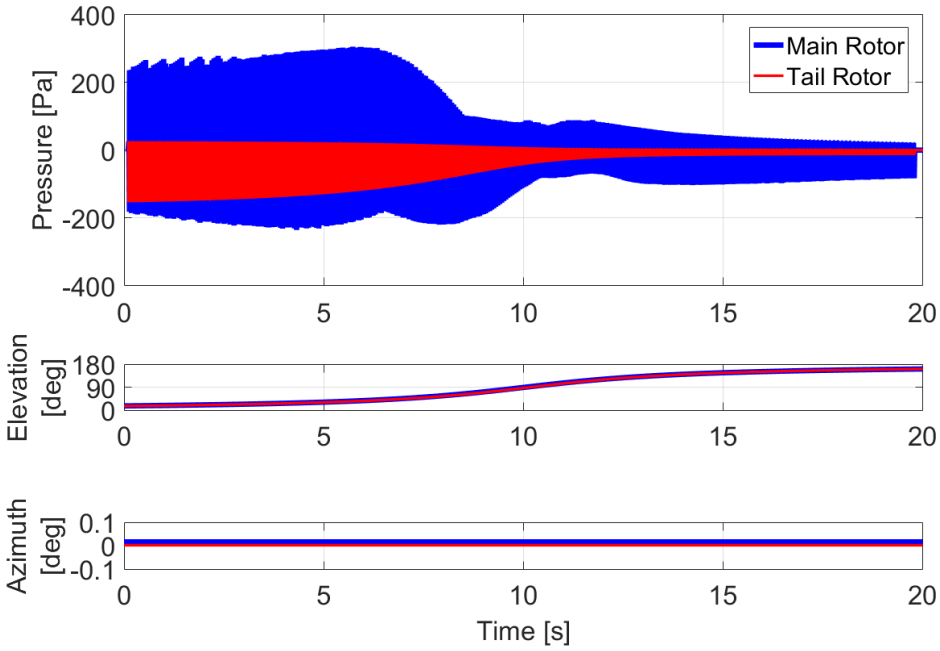

Figure 7. AS350 helicopter main and tail rotor F1A Synthesis.

A magnified view of the synthesized sound pressures from Figure 7 is shown in Figure 8. Here, the blade passages of the main and tail rotors can be seen more clearly. The main rotor BPF is approximately 19.8 Hz. The tail rotor BPF is approximately 70.0 Hz. The elevation emission angle is also magnified on the y-axis. The elevation emission angle difference between the main and tail rotor synthesis can also be seen more clearly. The main rotor blade passages have more fluctuation compared to the tail rotor blade passages. These fluctuations may be an artifact of the CAMRAD II data or the ANOPP2 F1A calculation, which will be commented on shortly.

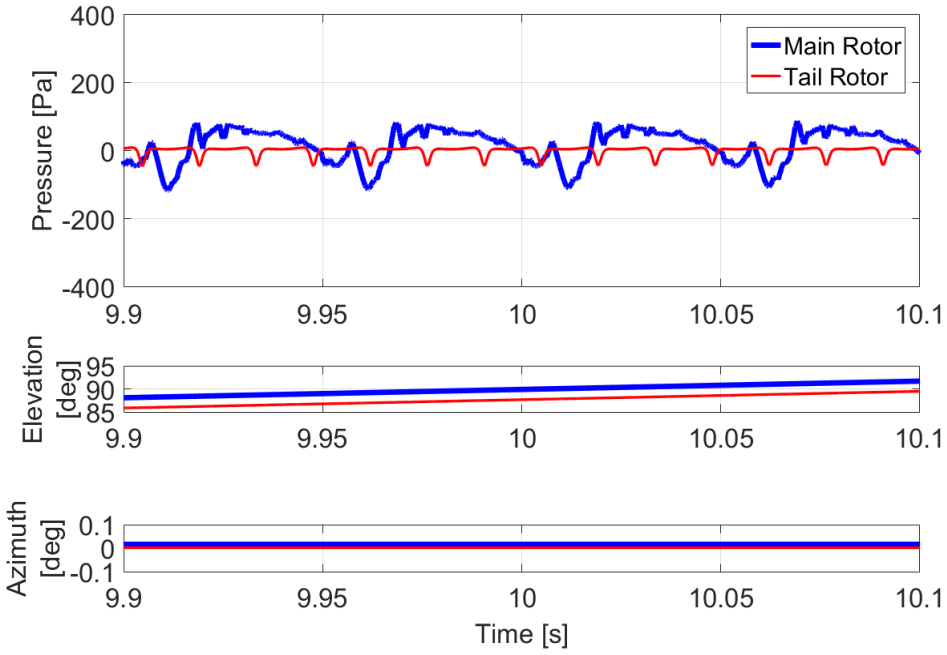

Figure 8. Magnified view of AS350 helicopter main and tail rotor F1A Synthesis.

Figure 9 shows spectrograms of the synthesized sound pressures. Since the F1A calculations occurred at the 8820 Hz sample rate, and the polyphase interpolator filters out frequencies above slightly less than half the tracking observer sample rate, there is little power above 4213 Hz. The tail rotor blade passage harmonics are more clearly discernible as horizontal lines compared with the main rotor harmonics. There is a time-frequency comb pattern in the main rotor spectrogram, especially at the lower frequencies, that obscures the harmonics. The comb pattern is described by similar magnitude levels that shift relatively smoothly in frequency over time to resemble an interference pattern. It is also present at lower magnitude and higher frequency in the main and tail rotor spectrograms. During propagation to a ground observer, the high frequency, low magnitude comb patterns in the tail rotor should be mitigated to some extent by atmospheric absorption.

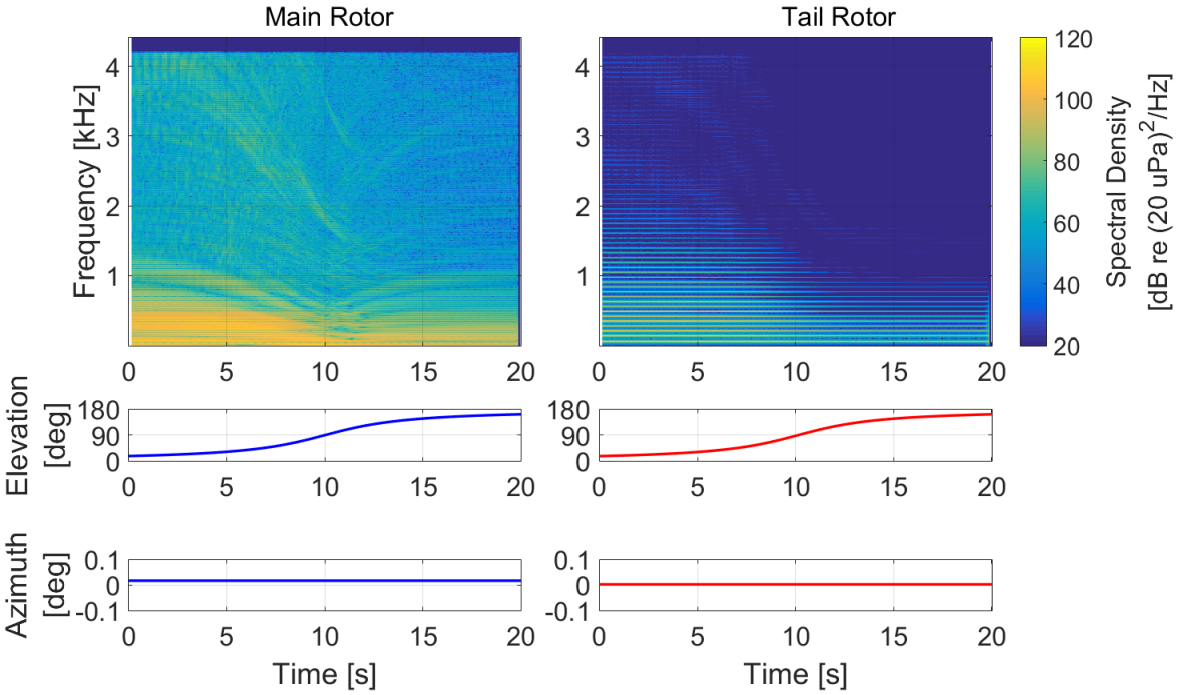

Figure 9. Spectrogram of AS350 helicopter main and tail rotor F1A Synthesis.

While a complete explanation of the comb pattern cannot yet be provided, some discussion of contributing factors can be made. Since the spectrogram data are at the tracking observer, the comb pattern is not interference from ground reflection. No Doppler effect is present because the tracking observer maintains a constant distance with the source emission track. Comb patterns also appear in the synthesis examples of Ref. [6], which used discrete source noise hemispheres and CAMRAD II BLMG data. It was explained in Ref. [6] that this pattern comes from the noise prediction and not the particular synthesis process.

C. Comparing F1A Synthesis with Additive Synthesis Using Discrete Data

The F1A Synthesis result is compared to additive synthesis using a discrete source noise hemisphere. Reference [6] showed convergence of the synthesized sound pressure of an AS350 helicopter main rotor time history as the discrete source noise hemisphere angular resolution became finer. The finest angular resolution attempted by Ref. [6] was 0.5 degrees. Therefore, periodic additive synthesis with 0.5 degree resolution is compared to the F1A Synthesis result. In this paper, only the main rotor synthesized sounds are compared.

For fair comparison with the F1A Synthesis result, convective amplification effects need to be added to the additive synthesis result. The F1A Synthesis includes the effects of convective amplification at the tracking observer. Although NAF additive synthesis adjusts the gain to account for spreading loss, convective amplification is not included because the discrete source noise hemisphere moves with the rotor during its F1A calculation of single blade passages.

Convective amplification is modeled and applied to the additive synthesized sound. A helicopter rotor can be decomposed into multiple radiating elements of noise. The convective amplification model for each element can be different based on their radiation pattern [14]. Since it will be challenging to determine a collective convective

amplification model by accounting for all radiating elements on a rotor, even for blades modeled as compact-lines, the radiation pattern of the entire main rotor is simplified to a monopole in this example calculation. Further, the azimuth emission angle of the main rotor to the ground observer is assumed to be approximately zero. With these assumptions, the convective amplification factor for the main rotor is modeled as a function of elevation emission angle, θ, by

$$C(\theta) = \frac{1}{1 - M\cos(\theta)}, 0° \le \theta \le 180° \tag{1}$$

In Equation (1), M is the Mach number of the vehicle/rotor. The amplitude of the additive synthesized sound is multiplied by Equation (1) to apply convective amplification. At the beginning of the flyover, when the elevation emission angle is closer to 0 degrees, the amplitude is increased by the convective amplification factor. Near the end of the flyover, when the emission angle is closer to 180 degrees, the amplitude is reduced by Equation (1).

Figure 10 compares the main rotor F1A Synthesis result and the additive synthesis result. The additive synthesis result is shown by the purple trace after filtering out frequencies above 4213 Hz and applying convective amplification. The additive synthesis result is offset from the F1A Synthesis result for clarity. The envelopes of the synthesized signals look similar. A spectrogram of the additive synthesis result is shown in Figure 11 alongside the F1A Synthesis result spectrogram from Figure 9. Although there are differences in the spectrograms, the comb pattern also appears in the additive synthesis result. Figure 11 confirms the result from Ref. [6] that the comb pattern is a result of the BLMG data from CAMRAD II or the F1A calculation, and not the particular sound synthesis process used.

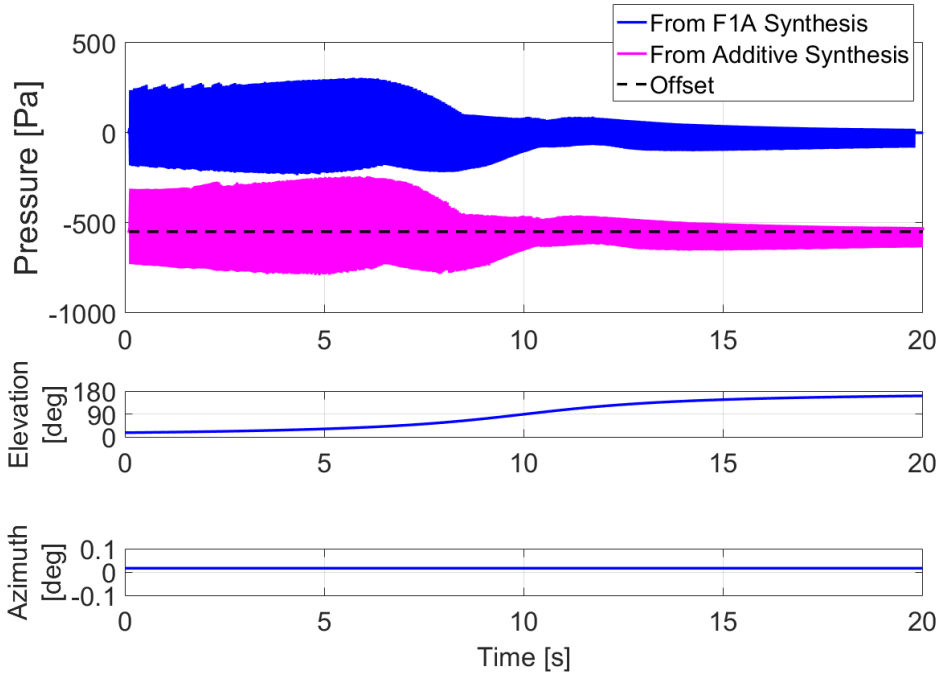

Figure 10. Comparing main rotor F1A Synthesis with periodic synthesis.

It should be noted that additional (polynomial) interpolation methods have recently been added to ANOPP2 to interpolate between emission and reception in an effort to mitigate these effects [23]. After applying these new interpolation methods, the main rotor synthesized pressure is decomposed into loading and thickness noise components (not shown for brevity). The comb pattern is present in the loading data but is not noticeable in the thickness data. When applying the interpolation method of linear extrapolation, as used in the previous work [11], the comb pattern is present in the thickness data. This result suggests that the comb pattern is at least partially formed by nonphysical effects. Other artifacts also appeared in the thickness data when applying the polynomial interpolation methods. Since the initial results using those methods are mixed, they are not used for the results in this paper. Instead, linear extrapolation was used to interpolate between emission and reception in the F1A calculation. Note also that the polyphase interpolator used in the NAF cannot interpolate unequally spaced time series data and is therefore not a candidate for use in the F1A calculation.

Sounds for the main rotor F1A Synthesis result and the additive synthesis result in Figures 10 and 11 are available online at Ref. [9]. The sounds are similar, but in the additive synthesis result, there are some high frequency sounds between three and seven seconds that are not present in the F1A Synthesis result. The additive synthesis result using a 0.5 degree resolution source noise hemisphere comes at significant computational cost. Significant memory and disk space resources are also needed to store blade passage calculations. Even with this cost, there are high frequency artifacts in the additive synthesized sound.

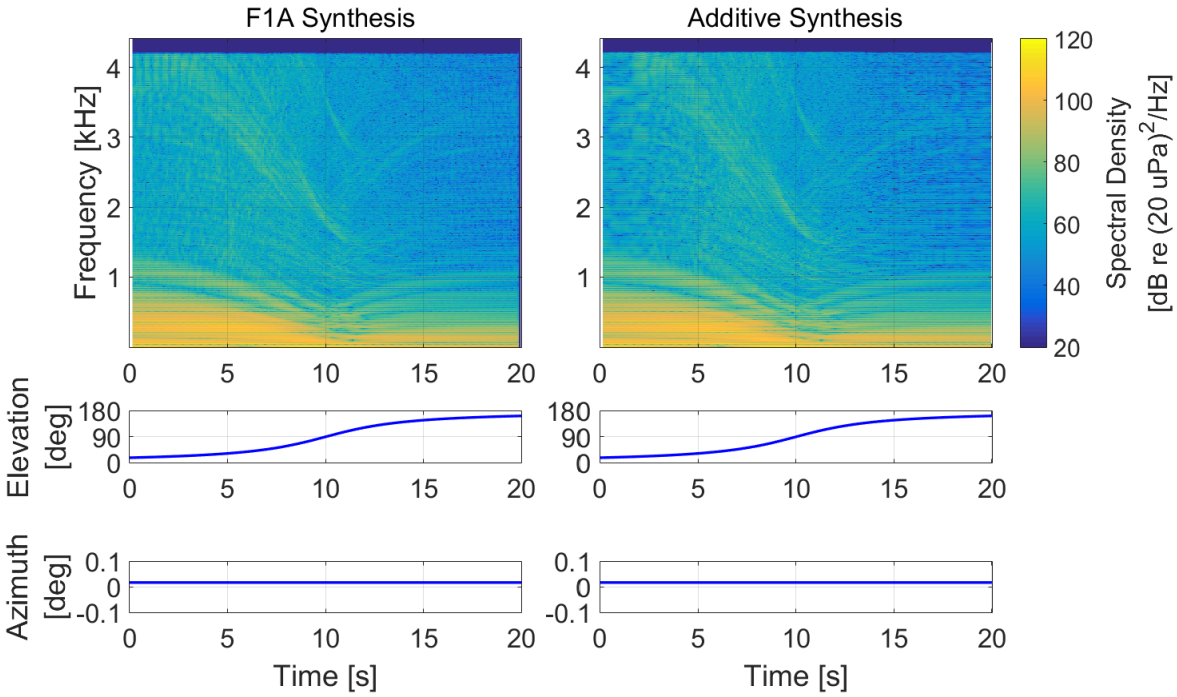

Figure 11. Spectrograms of main rotor F1A synthesis and periodic synthesis results.

D. Propagation to Ground Observer

After the synthesis process, the AS350 helicopter main and tail rotor tracking observer sound pressures are separately propagated to the ground observer as illustrated in Figure 6. Propagation proceeds in the NAF as described in Section III. After propagation, the main and tail rotor auralizations at the ground observer are combined to produce the pseudorecording. The results are shown in Figure 12. The black trace on the left is the sound pressure time history, and on the right is the corresponding spectrogram. The elevation and azimuth emission angle traces correspond to the emission angle between the ground observer and the vehicle center of gravity. The zero pressure at the beginning of the trace is the propagation delay to the ground observer. There is also an additional 0.1 second delay because the NAF was set to start the simulation at 0.1 seconds to allow sufficient time for initial buffers to be filled. Doppler frequency shifts are now present as seen in the spectrogram. Although the comb effect is still present, its magnitude is reduced at high frequencies relative to the magnitude of the synthesized sound. A sound file containing the auralized flyover is available online at Ref. [9].

Contributions from the main and tail rotors to the auralized sound are shown as spectrograms in Figure 13. Most of the auralized sound is due to the main rotor. Doppler effects on the tail rotor harmonics are more evident than on the main rotor. As indicated in Section V.B, comb effects at high frequencies in the tail rotor spectrogram are now mitigated relative to lower frequency harmonics as a result of atmospheric attenuation. Interference patterns at low frequencies in the tail rotor spectrogram are a result of spectral leakage in generating the spectrogram and can be mitigated using a different frequency resolution for the spectrogram.

This flyover example is considered to have just one propagation path from source emission position to ground observer for each rotor because the observer is flush with the ground. Nonetheless, in order to accurately capture the pressure doubling and accommodate elevated observers, the synthesized sounds are actually generated for two tracking observers each for the main and tail rotor. In the next example, the observer is not flush with ground and the generation of four tracking observers is clearer.

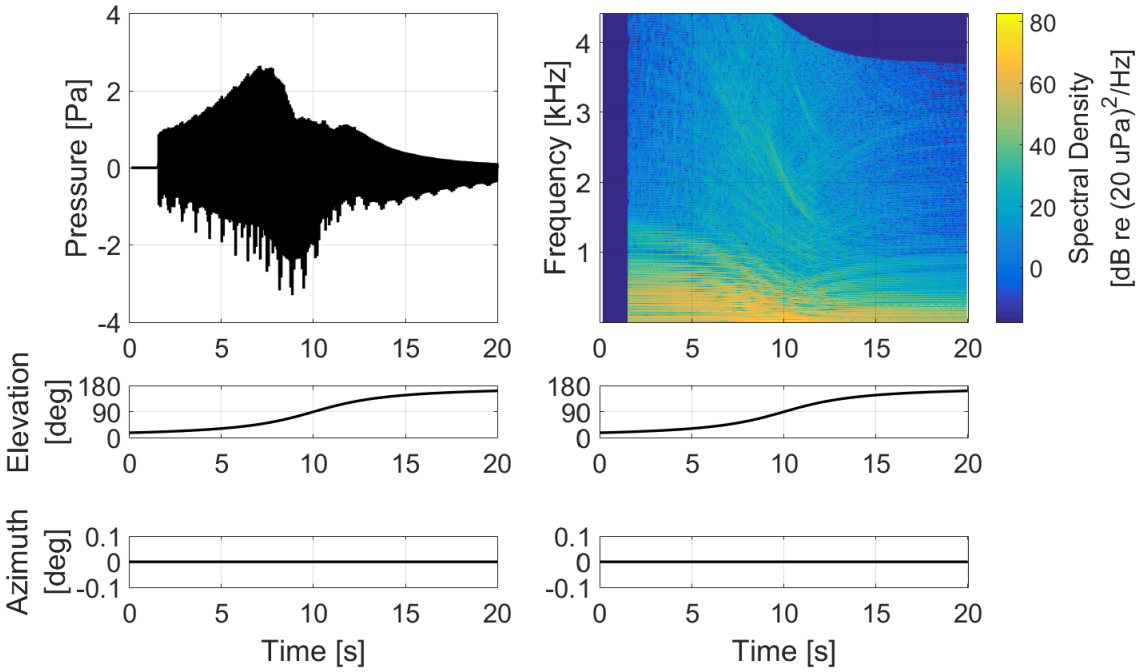

Figure 12. Auralized AS350 helicopter flyover.

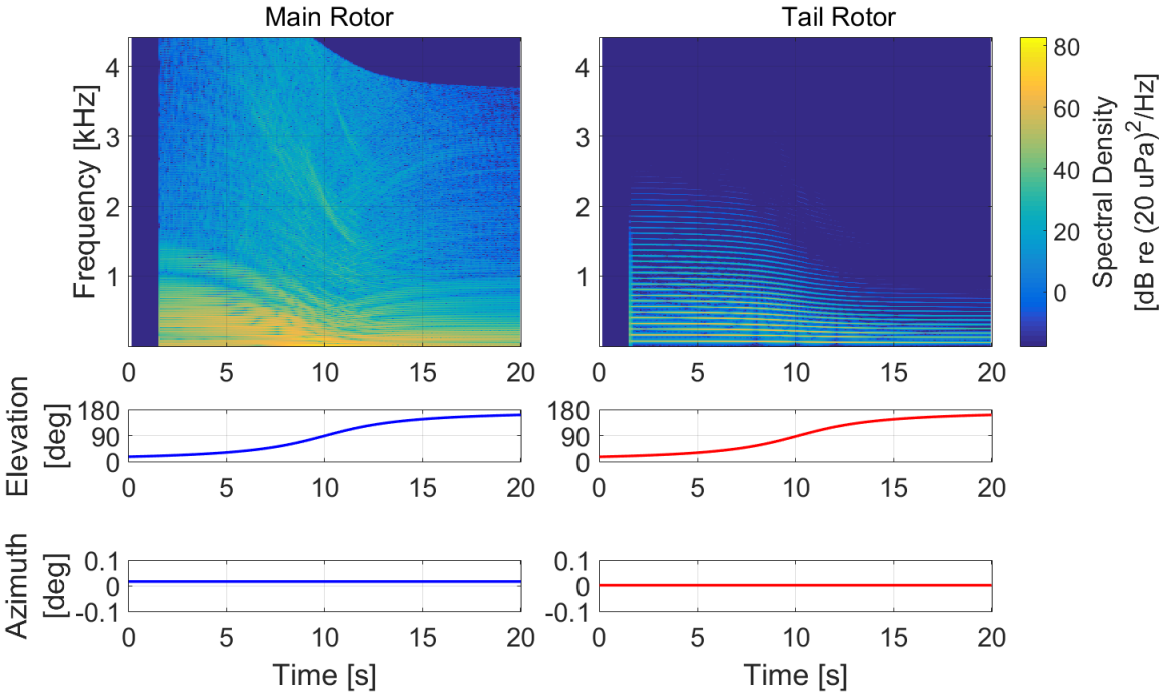

Figure 13. Auralized AS350 helicopter flyover, main and tail rotor contributions.

VI. Synthesis Example with Direct and Reflected Propagation Paths

A. Flyover Setup for Direct and Reflected Propagation Paths

Another example demonstrates the ability of the F1A Synthesis NAF plugin to handle multiple propagation paths. Starting with the same flyover setup as Figure 6, the ground observer is elevated 50 meters above the rigid ground as shown in Figure 14. This setup produces a different direct path and a reflected path from each rotor to the ground observer. Therefore, four unique tracking observers need to be created.

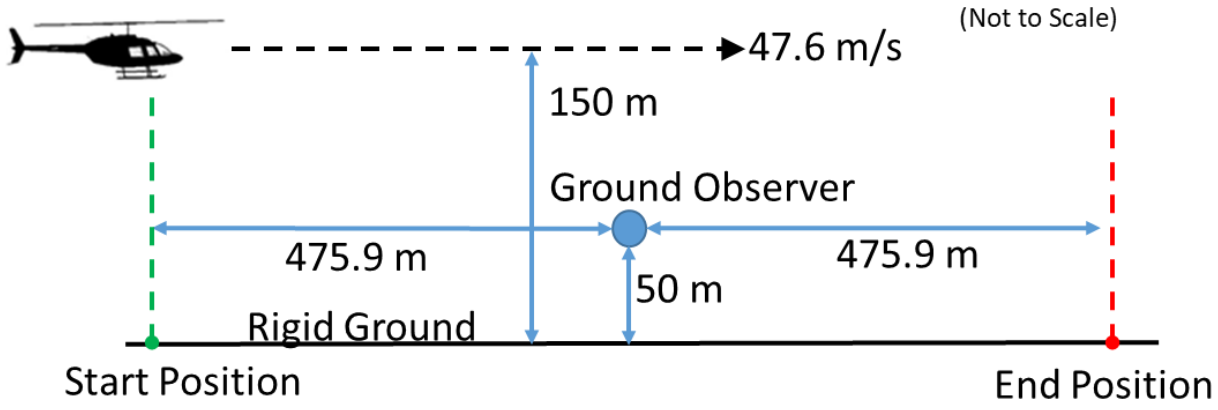

Figure 14. Flyover setup of synthesis example with direct and reflected propagation paths.

B. Synthesis and Propagation Results with Direct and Reflected Paths

Figure 15 shows the separate F1A Synthesis results. For each rotor, two results are given with different colored traces. One result is for the direct path from source emission position to ground observer and the other is for the ground reflected path. For each rotor, the synthesized sounds for the direct and reflected paths are visibly distinct because their tracking observers are formed from significantly different elevation emission angles. If a lower ground observer height was used, the synthesized sounds for the propagation paths will be less visibly distinct.

All four tracking observer results are propagated using the NAF and combined at the ground observer. Figure 16 shows the results. The black trace on the left is the auralized time history and the corresponding spectrogram is shown on the right. The elevation and azimuth emission angle traces are for the direct path between the vehicle center of gravity and the ground observer. As a result of the synthesized sounds' direct and reflected paths being substantially different from each other (compared to sounds synthesized for paths with closely spaced emission angles), a prominent interference pattern due only to ground reflection is not apparent in the auralized spectrogram. A sound file containing this auralized flyover is available online at Ref. [9].

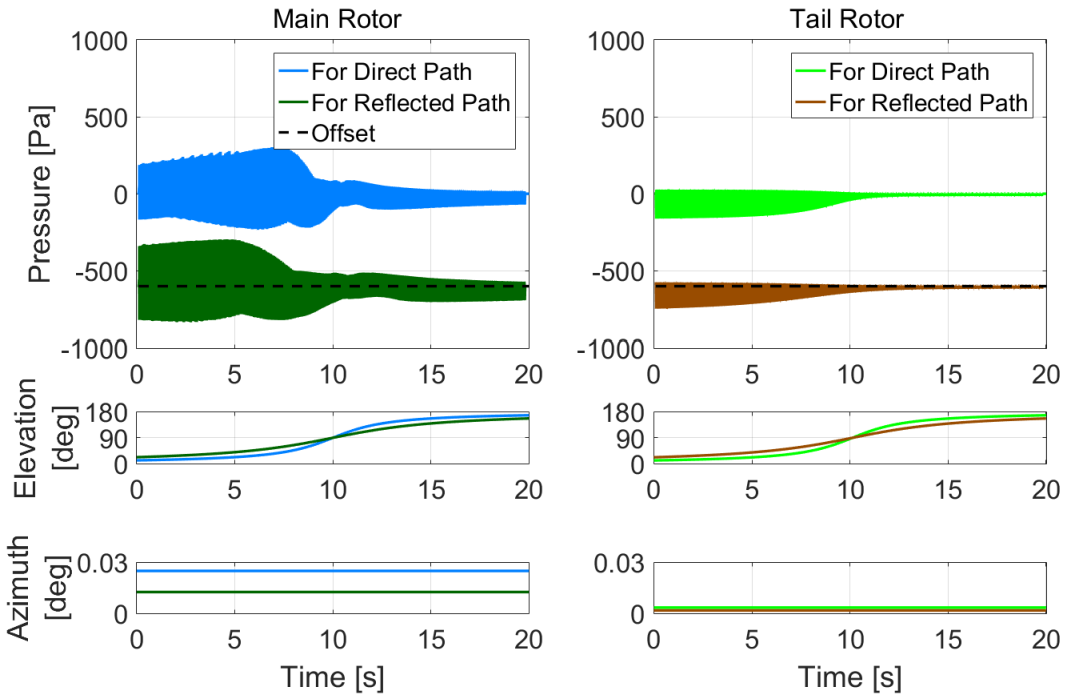

Figure 15. F1A Synthesis at tracking observers for direct and reflected paths of AS350 helicopter main and tail rotors.

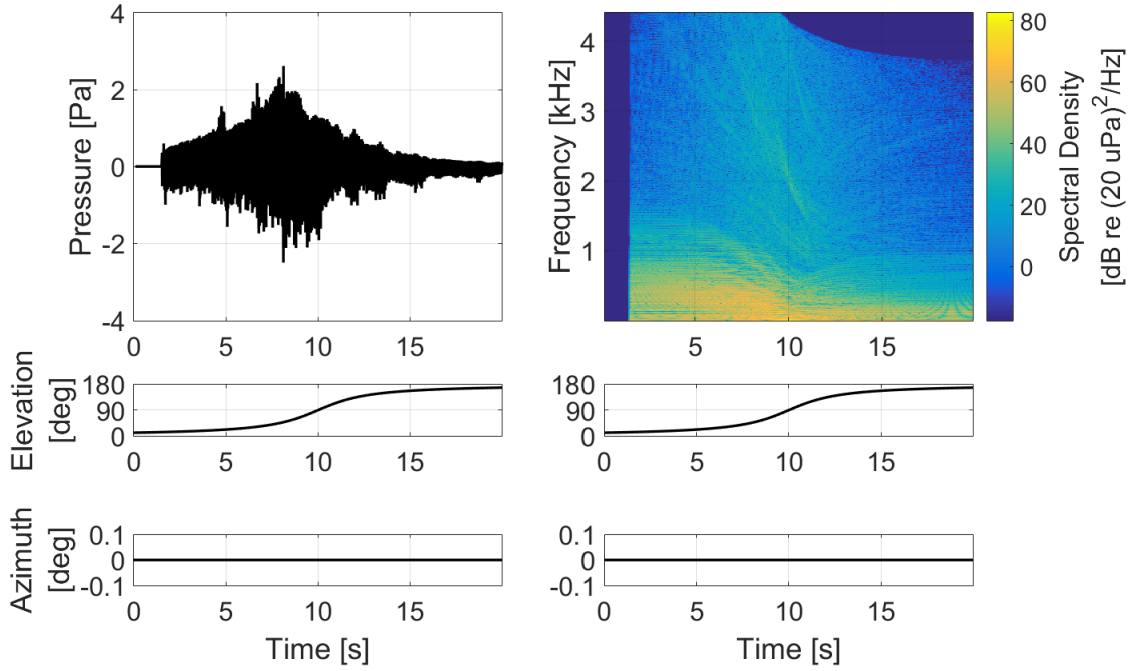

Figure 16. Auralized AS350 helicopter flyover at 50 m ground observer.

VII. Conclusions

This paper demonstrates implementation of F1A Synthesis into a NAF plugin. The F1A Synthesis Preprocessor architecture is described. The preprocessor generates a separate source emission track and tracking observer for each noise source, or rotor. Additional tracking observers are generated for additional propagation paths. Two successful AS350 helicopter main and tail rotor flyover synthesis examples are provided to demonstrate the preprocessor. The first example uses an observer flush with the ground. The second example uses an observer above ground to generate visibly distinct pressure time histories for direct and reflected propagation paths. For both examples, the synthesized sounds are of a steady periodic source with blade loading data provided by CAMRAD II. An unsteady or aperiodic auralization can be generated using the process described here if unsteady or aperiodic blade loadings are provided as input. Synthesized main rotor sound pressure from F1A Synthesis are compared to the sound pressure generated by an earlier additive synthesis method. High frequency audible artifacts present in the additive synthesis result and not found in the F1A Synthesis result, demonstrating the superiority of the F1A method.

Comb effects in the synthesized sound spectrograms are discussed. While a full explanation for the comb effects is not known at this time, this paper confirms an earlier hypothesis that these effects originate either from the BLMG data or from the F1A calculation within ANOPP2, and not an artifact of either the additive synthesis or F1A Synthesis methods. Improvements to interpolation methods used by ANOPP2 between source emission and observer reception pressures may mitigate the comb effects, but a more detailed investigation is required.

Additional work is required to bring the constituent F1A Synthesis components together into a single NAF advanced plugin library. A demonstration of the ability of the plugin to handle unsteady blade loadings is also needed to identify any implementation issues. Support for ANOPP2'a new ABEAT tool for propeller noise will allow greater utilization of the F1A Synthesis capability for propeller noise studies.

VIII. Acknowledgements

The authors thank Leonard V. Lopes of NASA Langley Research Center, Jeremy J. Jones of Analytical Mechanics Associates, and Doug D. Boyd of NASA Langley Research Center for their assistance and software updates to ANOPP2 that allowed F1A Synthesis to be successfully run. Also thanks to Aric R. Aumann of Science Applications International Corp. for his assistance with running the NAF. This work was performed with support from the Revolutionary Vertical Lift Technology Project of the NASA Advanced Air Vehicles Program.

IX. References

[1] A. R. Aumann, B. C. Tuttle, W. L. Chapin and S. A. Rizzi, "The NASA Auralization Framework and plugin architecture," in *InterNoise 2015*, San Francisco, CA, USA, 2015.

[2] M. Vorländer, Auralization - Fundamentals of Acoustics, Modelling, Simulation, Algorithms and Acoustic Virtual Reality, Springer-Verlag Berlin Heidelberg, 2008.

[3] S. A. Rizzi and A. K. Sahai, "Auralization of air vehicle noise for community noise assessment," *CEAS Aeronautical Journal,* vol. 10, pp. 313-334, 3 2019.

[4] F. Farassat and G. P. Succi, "The Prediction of Helicopter Rotor Discrete Frequency Noise," *Vertica*, vol. 7, pp. 309-320, 1983.

[5] J. E. F. Williams and D. L. Hawkings, "Sound Generation by Turbulence and Surfaces in Arbitrary Motion," *Philosophical Transactions of the Royal Society of London. Series A, Mathematical and Physical Sciences,* vol. 264, pp. 321-342, 1969.

[6] S. Krishnamurthy, S. A. Rizzi, D. D. Boyd and A. R. Aumann, "Auralization of Rotorcraft Periodic Flyover Noise from Design Predictions," in *Proceedings of the 74th Annual Forum, American Helicopter Society International*, Phoenix, AZ, 2018.

[7] A. Christian, D. D. Boyd, N. S. Zawodny and S. A. Rizzi, "Auralization of tonal rotor noise components of a quadcopter flyover," in *InterNoise 2015*, San Francisco, CA, USA, 2015.

[8] S. Krishnamurthy, B. C. Tuttle and S. A. Rizzi, "Auralization of Unsteady Rotor Noise using a Solution to the Ffowcs Williams- Hawkings Equation," in *Proceedings of the 75th Annual Forum, Vertical Flight Society*, Philadelphia, 2019.

[9] "Aircraft Flyover Simulation," 2020. [Online]. Available: https://stabserv.larc.nasa.gov/flyover/.

[10] E. Greenwood, F. H. Schmitz and R. D. Sickenberger, "A Semiempirical Noise Modeling Method for Helicopter Maneuvering Flight Operations," *Journal of the American Helicopter Society,* vol. 60, pp. 1-13, 2015.

[11] L. V. Lopes and C. L. Burley, "ANOPP2 User's Manual," NASA/TM-2016-219342, Hampton, VA, 2016.

[12] S. Krishnamurthy and S. A. Rizzi, "Auralization of Amplitude Modulated Helicopter Flyover Noise," in *AIAA Scitech 2019 Forum, AIAA 2019-2087*, San Diego, CA, 2019.

[13] A. Christian and J. Lawrence, "Initial Development of a Quadcopter Simulation Environment for Auralization," in *Proceedings of the 72nd Annual Forum, American Helicopter Society International*, West Palm Beach, FL, 2016.

[14] A. Dowling, "Convective amplification of real simple sources," *Journal of Fluid Mechanics,* vol. 74, pp. 529-546, 1976.

[15] K. S. Brentner, L. V. Lopes, H.-N. Chen and J. F. Horn, "Near Real-Time Simulation of Rotorcraft Acoustics and Flight Dynamics," *Journal of Aircraft,* vol. 42, pp. 347-355, 2005.

[16] G. Perez, K. S. Brentner, G. A. Brès and H. E. Jones, "A First Step Toward the Prediction of Rotorcraft Maneuver Noise," *Journal of the American Helicopter Society,* vol. 50, pp. 230-237, 2005.

[17] H.-N. Chen, K. S. Brentner, L. V. Lopes and J. F. Horn, "An Initial Analysis of Transient Noise in Rotorcraft Maneuvering Flight," *International Journal of Aeroacoustics,* vol. 5, pp. 109-138, 4 2006.

[18] H. Chen, nien, K. S. Brentner, S. Ananthan and J. G. Leishman, "A Computational Study of Helicopter Rotor Wakes and Noise Generated During Transient Maneuvers," *Journal of the American Helicopter Society,* vol. 53, pp. 37-55, 2008.

[19] M. Arntzen, S. A. Rizzi, H. G. Visser and D. G. Simons, "Framework for Simulating Aircraft Flyover Noise Through Nonstandard Atmospheres," *Journal of Aircraft,* vol. 51, pp. 956-966, 5 2014.

[20] W. Johnson, "Comprehensive Analytical Rotorcraft Model of Rotorcraft Aerodynamics and Dynamics, Version 4.10," in *Johnson Aeronautics, Volumes I-9*, 2017.

[21] L. C. Nguyen and J. J. Kelly, "A Users Guide for the NASA ANOPP Propeller Analysis System," NASA Contractor Report 4768, Hampton, VA, 1997.

[22] R. E. Crochiere and L. R. Rabiner, Multirate Digital Signal Processing, B. Cassel and M. Carnis, Eds., Prentice-Hall, Inc., 1983.

[23] L. V. Lopes, "ANOPP2's Farassat's Formulations Internal Functional Module (AFFIFM) Reference Manual," Version 1.3 ed., NASA Langley Research Center, Hampton, VA 23681, NASA, 2020, pp. 35-36.